Available online at www.sciencedirect.com
SCIENCE DIRECT®
International Journal of Thermal Sciences 42 (2003) 1013–1020
International Journal of Thermal Sciences
www.elsevier.com/locate/ijts

Experimental investigation of the influence of buoyancy on turbulent flow adjacent to a horizontal plate induced by a trip wire

H.I. Abu-Mulaweh

Mechanical Engineering Department, Purdue University at Fort Wayne, Fort Wayne, IN 46805, USA

Received 9 October 2002; accepted 17 February 2003

Abstract

The effects of buoyancy force on fully developed turbulent mixed convective boundary layer flow over a horizontal heated flat plate are studied experimentally. A 4-mm trip wire, placed 10 cm from the leading edge of the plate, was used for accelerating the flow transition from laminar to turbulent. Measurements of the flow field were carried out at two streamwise locations ($x = 125$ and 150 cm), for two free stream velocities of $u_\infty = 1.15$ and $2\ \mathrm{m\cdot s^{-1}}$, and four different temperature differences between the heated surface and the free stream air: $\Delta T = 0\,^\circ\mathrm{C}$ (i.e., forced convection) and $\Delta T = 15$, 30, and $53\,^\circ\mathrm{C}$ (i.e., mixed convection) by using a laser-Doppler velocimeter. The measured results are compared with results from turbulent flow theory. The results revealed, as expected, the trip wire did accelerate the transition of laminar boundary layer flow to a fully developed turbulent boundary layer flow. Also, it was found that the buoyancy force resulting from wall heating has negligible effect on the flow field as long as the flow is stable because the buoyancy force has no streamwise component

1. Introduction

Turbulent convective flow adjacent to horizontal heated flat plate is encountered in a wide variety of heat transfer engineering applications and environmental situations. Many investigations have, therefore, been carried out to examine its characteristics. The effects of buoyancy force on turbulent boundary layer flow over a heated horizontal flat plate were examined analytically by many investigators (see, for example, [1–4], and the references cited therein). Experimental results on turbulent mixed convection from heated horizontal surfaces were reported by Townsend [5] for air flow and by Imura et al. [6] and Cheng et al. [7] for water flow. The experimental results of Townsend [5] showed that the mean velocity and mean temperature distributions were closely similar, implying that a close analogy for the transfer coefficient of momentum and heat in the boundary layer. Imura et al. [6] have found that for the Reynolds number range of $3.2 \times 10^3 \leqslant Re_x \leqslant 2 \times 10^5$, the transition from laminar forced convection to turbulent mixed convection occurs when $100 < Gr_x/Re_x^{1.5} < 300$, and that the heat transfer rates become independent of Reynolds number for $Gr_x/Re_x^{1.5} > 300$. Cheng et al. [7] extended the work of Imura et al. [6] to higher Reynolds numbers ($2.5 \times 10^4 \leqslant Re_x \leqslant 2.2 \times 10^6$). They found that for $Gr_x/Re_x^{1.5} > 200$, the heat transfer rate becomes higher than the turbulent free convection value.

The development of fully turbulent mixed convection flow in a laboratory can be limited, however, by the magnitude of the free stream velocity, the length of the plate and the temperature difference between the plate and the free stream. To overcome these constraints, a trip wire can be used at or near the leading edge of the plate to accelerate the flow transition from laminar to turbulent flow. Miau and Chen [8] have utilized a trip wire to thicken the boundary layer to study the flow structures behind a vertically oscillating fence immersed in a flat-plate turbulent boundary layer. Ziugzda and Tonkonogiy [9] employed longitudinal baffle to achieve turbulent flow at low Reynolds number. Recently, Carpinlioglu [10] and Pinson and Wang [11] examined the effects of leading edge roughness on the flow and thermal fields in the transitional boundary layer over a flat surface.

The purpose of this investigation is to study experimentally the characteristics of the flow field of a mixed turbulent convection flow generated by a trip wire placed near the leading edge of the plate. Moreover, the effects of buoyancy forces on turbulent mixed convection boundary layer flow adjacent to a horizontal, heated flat plate that is maintained at constant temperature are also examined. Measurements

E-mail address: mulaweh@engr.ipfw.edu (H.I. Abu-Mulaweh).

1290-0729/$ – see front matter
doi:10.1016/S1290-0729(03)00078-4

Nomenclature

C_{fx}	local friction factor $= \tau_w/(\rho u_\infty^2/2)$	
g	gravitational acceleration	$\mathrm{m \cdot s^2}$
Gr_x	local Grashof number $= g\beta(T_w - T_\infty)x^3/\nu^2$	
Re_x	local Reynolds number $= u_\infty x/\nu$	
T_f	film temperature $= (T_w + T_\infty)/2$	°C
T_w	wall temperature	°C
T_∞	free stream temperature	°C
u	time-averaged velocity	$\mathrm{m \cdot s^{-1}}$
u'	instantaneous velocity fluctuation from the mean	$\mathrm{m \cdot s^{-1}}$
u^*	friction velocity $= (\tau_w/\rho)^{1/2}$	$\mathrm{m \cdot s^{-1}}$
u_∞	free stream velocity	$\mathrm{m \cdot s^{-1}}$
u^+	dimensionless velocity $= u/u^*$	
x, y	axial and normal coordinates	m
y^+	dimensionless distance from the wall, $= yu^*/\nu$	

Greek symbols

β	volumetric coefficient of thermal expansion, $= 1/T_f$	$\mathrm{°C^{-1}}$
δ	hydrodynamic boundary layer thickness	mm
ΔT	temperature difference, $= T_w - T_\infty$	°C
ν	kinematic viscosity	$\mathrm{m^2 \cdot s^{-1}}$
τ_w	wall shear stress, $= \mu(\partial u/\partial y)_{y=0}$	$\mathrm{kg \cdot m^{-1} \cdot s^{-2}}$
ρ	fluid density	$\mathrm{kg \cdot m^{-3}}$

of turbulent velocity profiles and velocity fluctuations were performed in the boundary layer at different downstream locations for different free stream velocities and different plate temperatures by employing a laser-Doppler velocimeter (LDV).

2. Experimental apparatus and procedure

The experimental investigation was carried out in a low-turbulence, open-circuit air tunnel that was horizontally oriented, as shown schematically in Fig. 1. The tunnel consisted of a smooth converging nozzle, a test section, and a smooth diverging diffuser. This tunnel is similar to the one described by Abu-Mulaweh et al. [12], with a test section length of 2.2 meters. The test section, which is constructed from transparent Plexiglas material, allows for flow visualizations and permits the use of a laser-Doppler velocimeter (LDV) for velocity measurements. The heated flat plate (200 cm long) is supported in the test section of the tunnel and spans its entire width (30.48 cm) and it can be heated to a constant and uniform temperature. The heated plate was constructed of four layers which were held together by screws and instrumented to provide an isothermal heated surface. The upper layer was an aluminum plate (1.27 cm thick) instrumented with several thermocouples that are distributed in the axial direction along its entire length. Each thermocouple was inserted into a small hole from the back of the plate and its measuring junction was flush with the test surface. The second layer consisted of several heating pads that can be controlled individually for electrical energy input. By controlling the level of electrical energy input to each of the heating pads, and monitoring the local temperature of the heated surface with imbedded thermocouples, the temperature of the heated plate can be maintained constant and uniform to within 0.2 °C. An insulation layer formed the third layer. The bottom layer was an aluminum plate which served as backing and support for the heated wall structure. The plate temperature could be maintained at a uniform and constant value in the range of 25 to 90 °C and the free stream velocity in the tunnel could be varied between 0.3 and 3 $\mathrm{m \cdot s^{-1}}$. The average velocity and the instantaneous velocity deviation from the mean were measured at various axial locations by employing a single-channel laser-Doppler velocimeter (LDV) using a counter as the Doppler signal processor. The LDV was mounted on a three-dimensional traversing system

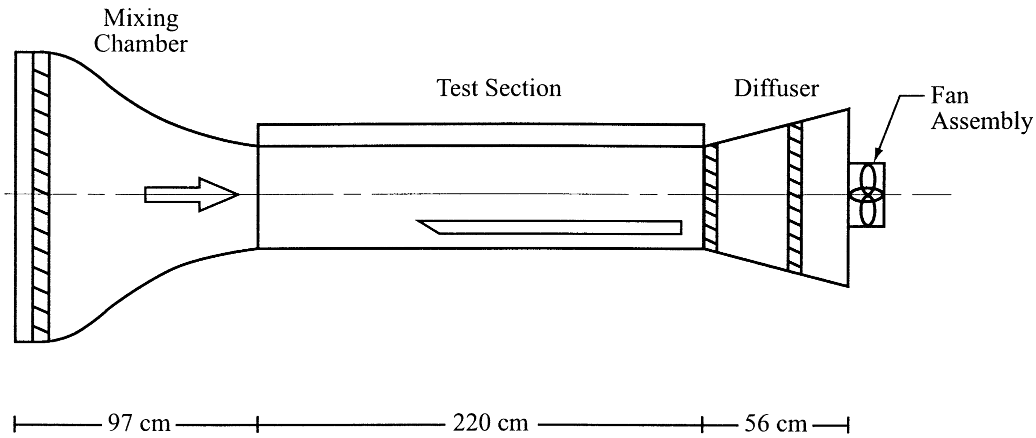

Fig. 1. Schematic diagram of the air tunnel.

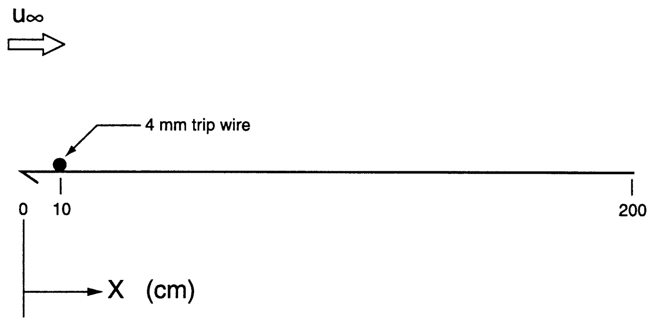

Fig. 2. Horizontal flat plate with trip wire.

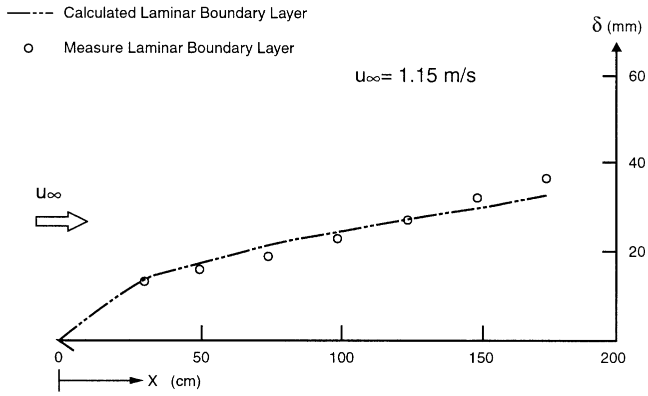

Fig. 3. Development of momentum laminar boundary layer.

capable of placing the measuring volume of the LDV at any x, y, z location in the flow within accuracies of 0.05, 0.003, and 0.05 mm, respectively.

It was established, through repeated LDV measurements, that 128 acceptable LDV samples of the local instantaneous fluctuating velocity component were sufficient to repeatedly and accurately determine the local mean velocity in the flow domain. The acceptable sampling rate for these measurements varied between 5 and 30 sample·sec^{-1}.

Flow visualizations were also performed to verify the boundary-layer development and its two-dimensional nature. These flow visualizations were carried out by using a 15-Watt collimated white light beam, 2.5 cm in diameter. Glycerin smoke particles, 2 to 5 microns in diameter, which are generated by immersing a 100 Watt heating element into a glycerin container, are added to the inlet air flow and used as scattering particles for flow visualization and for LDV measurements.

Due to the limited length of the test section, the flat plate, and the magnitude of the velocity, a fully turbulent mixed convection flow could not be achieved experimentally in our laboratory. To overcome this limitation a trip wire with a diameter of 4 mm was used to trigger the flow and to accelerate the flow transition from laminar to turbulent mixed convection flow. The trip wire was placed flush with the surface of the plate at a distance of 10 cm from the leading edge as shown in Fig. 2. The thermophysical properties that were used in the calculations were evaluated at the average film temperature.

The repeatability of the mean velocity measurements was determined to be within 3 percent, and that of the temperature measurements was within 0.2 °C (0.5%). The uncertainties in the measured results were estimated (at the 95% confidence level) according to the procedure outlined by Moffat [13] and they are reported in the appropriate section of this paper.

3. Experimental results and discussion

The air flow boundary layer development in the experimental set up, along with its two-dimensional nature, was verified through flow visualization and through measurements of velocity across the width of the tunnel, at several heights above the heated flat plate. These measurements showed a wide region (about 80% of the width of the heated wall around its center $z = 0$) where the air flow velocity, in the z direction at a fixed distance from the heated wall, could be approximated (to within 4%) as uniform and two-dimensional flow.

The operation of the air tunnel, its instrumentation, along with the accuracy and the repeatability of the measurements were validated by measuring velocity distributions of laminar forced convection boundary-layer flow adjacent to unheated flat plate (without the trip wire) for different free stream velocities and streamwise locations. The measurements were in good agreement with the predicted values (Blasius solution), with deviations of less than 2%, thus validating the performance of the air tunnel and its instrumentations. All reported velocity and temperature measurements were taken along the midplane ($z = 0$) of the plate's width, and only after the system had reached steady-state conditions.

Measurements of the hydrodynamic laminar boundary layer thickness along the unheated horizontal flat plate without the aid of the trip wire for the case of isothermal flow with free stream velocity of $u_\infty = 1.15\ \mathrm{m{\cdot}s^{-1}}$ is shown in Fig. 3. The calculated laminar boundary layer thickness is also shown in the figure (dashed line) for comparison. As can be seen clearly from the figure, the measured thickness of the laminar boundary layer agrees well with that of the calculated value. The boundary layer thickness was determined by scanning the velocity profile normal to the test surface, and by identifying the location where the average velocity is equal to the free stream velocity, i.e., $y = \delta$ when $u = u_\infty$.

The measured thickness of the hydrodynamic turbulent boundary layer which was developed with the aid of the trip wire, is compared in Fig. 4 with the boundary layer thickness that is calculated using the following relation:

$$\delta/x^* = 0.371 Re^{*-1/5} - 2229\, Re^{*-1} \qquad (1)$$

where $x^* = x_0 + x$ and $Re^* = x^* u_\infty/\nu$, with x_0 denoting the artificial leading length that is required to make the calculated boundary layer thickness to agree with the measured

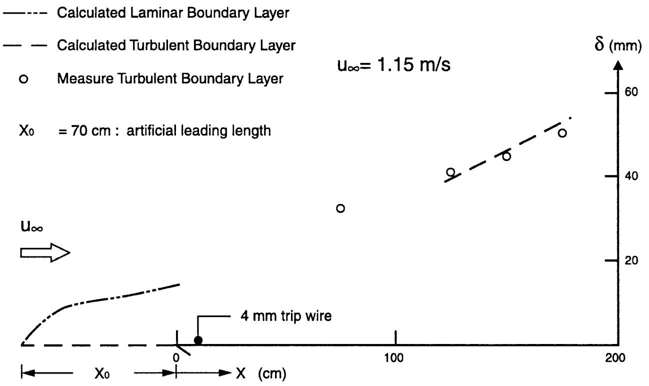

Fig. 4. Development of momentum turbulent boundary layer.

boundary layer thickness. The value of x_0 was determined to be 70 cm ahead of the plate. The derivation of Eq. (1) is similar to that given in Holman [14] with a critical turbulent Reynolds number equal to 1×10^5. Without the use of a trip wire, the critical turbulent Reynolds number used by Holman is 5×10^5. In the present experimental study, in which a trip wire was used for accelerating the flow transition from laminar to turbulent flow, it was found that the critical turbulent Reynolds number decreased to a value equal to 1×10^5 at which transition from laminar to turbulent flow occurs. The effectiveness of the trip wire in accelerating the transition of laminar boundary layer flow to turbulent boundary layer flow can be seen clearly from Fig. 4 through the rapidly increasing thickness of the momentum boundary layer after the trip wire.

The measured velocity profiles for flow over an unheated horizontal flat plate with and without a trip wire for free stream velocities of 1.l5 and 2.0 $\text{m}\cdot\text{s}^{-1}$ are presented, respectively, in Fig. 5 for several values of downstream location. The uncertainty in the measured u/u_∞ is ±3% and in y/δ is 2%. It is seen that without the aid of the trip wire, the velocity profiles at $x = 30$ and 75 cm agree well with the Blasius profile. On the other hand, the velocity profiles at $x = 150$ and 175 cm deviate from the Blasius profile. This indicates that the flow at these axial locations is no longer a laminar flow, and it is probably the start of the transition to the turbulent boundary layer flow. It is also clear from these two figures that with a trip wire, the velocity profiles at axial locations that are greater than 125 cm agree with that of 1/7th power law:

$$u/u_\infty = (y/\delta)^{1/7} \tag{2}$$

which is normally associated with a fully developed turbulent boundary layer flow. This figure clearly indicates that the rate of approaching the fully turbulent velocity profile increases as the free stream velocity and the distance from the leading edge increase. The measured boundary layer thickness, δ, was used in the dimensionless parameter, y/δ, that appears in Fig. 5.

Unlike the unheated horizontal boundary layer flow in which the laminar flow experiences a transition to turbulent flow through wave instability, the heated laminar boundary

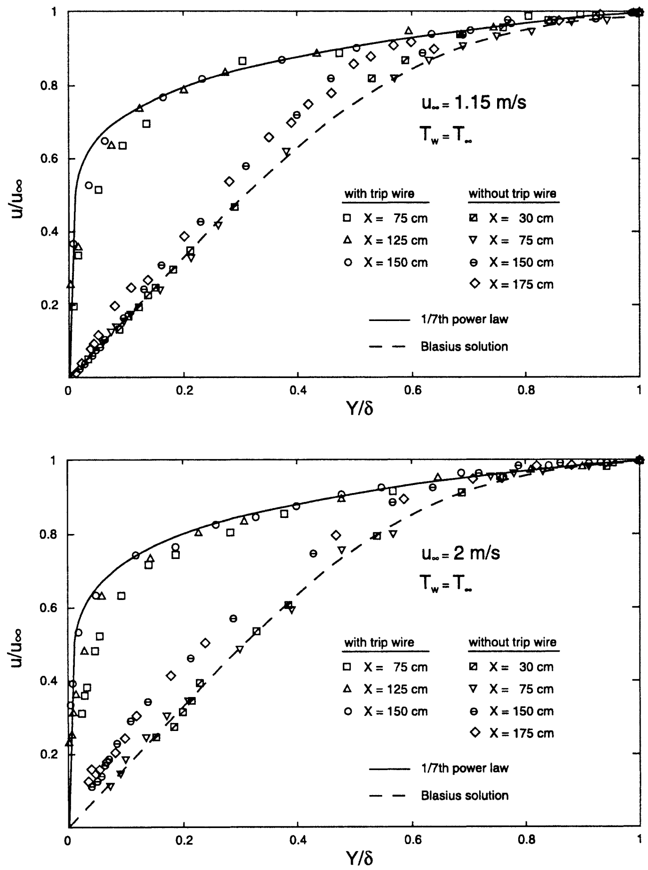

Fig. 5. Comparison between measured and predicted velocity distributions for an unheated plate with and without a trip wire: (a) $u_\infty = 1.15\ \text{m}\cdot\text{s}^{-1}$, (b) $u_\infty = 2\ \text{m}\cdot\text{s}^{-1}$.

layer flow can experience a transition to turbulent flow through thermal or vortex instability. In some cases the vortex instability occurs earlier than the wave instability and for that reason heated boundary layer flow can experience an earlier transition from laminar to turbulent flow than the unheated flow case, as shown in Fig. 6. The vortex instability causes the onset of longitudinal vortices in the flow. This causes a breakdown in the two-dimensional nature of the flow and transforms it to a three-dimensional flow, in which the vortices develop and grow until they breakdown, thus developing into a two-dimensional turbulent flow domain. The incipience and growth of vortex rolls in boundary layer flow adjacent to horizontal heated flat plate was examined in detail by Moharreri et al. [15] who reported the following relation for the onset of the vortex instability:

$$Gr_x = 100 Re_x^{1.5} \tag{3}$$

This relation can be used to establish the axial location at which the vortex instability starts under a given free stream velocity and a given temperature difference between the heated plate and the free stream. For example, the solid lines in Fig. 7 show the effect of free stream velocity on the onset/start of instability and flow transition for an unheated horizontal boundary layer flow. The start of the wave instability and transition to turbulent flow is selected as

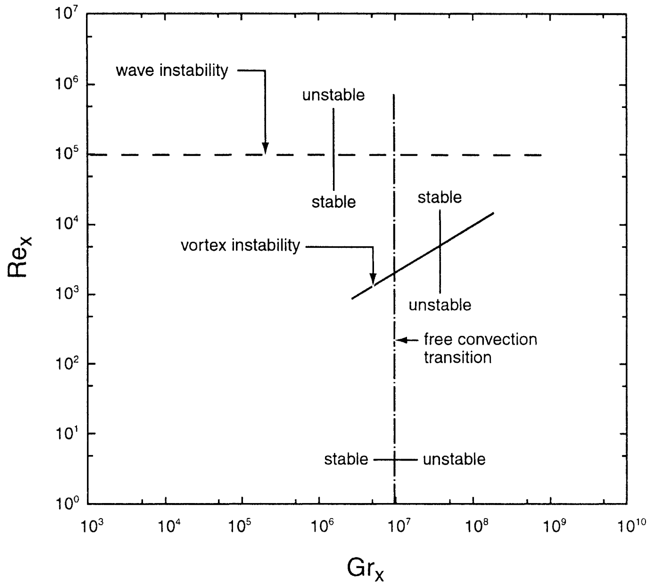

Fig. 6. Vortex and wave instability regimes.

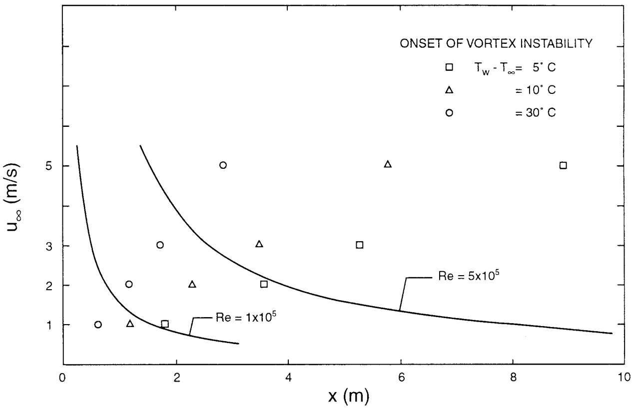

Fig. 7. Effect of free stream velocity and temperature difference on the onset of instability.

Reynolds number, $Re_{x,c} = 1 \times 10^5$, and the fully developed turbulent flow is selected as, $Re_{x,c} = 5 \times 10^5$. Thus, for a given free stream velocity, the downstream axial location for the transition can be determined. Fig. 7 clearly indicates that the length of both the stable region for ($Re_x \leqslant 1 \times 10^5$) and the unstable region for ($1 \times 10^5 \leqslant Re_x \leqslant 5 \times 10^5$) decrease as the free stream velocity increases. The figure also shows the locations where vortex instability starts under a given free stream velocity and a given temperature difference between the heated plate and the free stream as calculated form Eq. (3). It is clear from this figure that vortex instability could be the cause for initiating the transition from laminar to turbulent flow. Vortex instability will significantly influence the flow if it occurs before the onset of wave instability (i.e., for $Re_x \leqslant 1 \times 10^5$).

To examine the effect of buoyancy force on turbulent forced convection adjacent to a horizontal flat plate induced by a trip wire, measurements of the flow field were carried out at two streamwise locations ($x = 125$ and 150 cm), for two free stream velocities of $u_\infty = 1.15$ (corresponding to Reynolds numbers $Re_x = 8.98 \times 10^4$ and 1.08×10^5, respectively) and $u_\infty = 2\ \mathrm{m{\cdot}s^{-1}}$ (corresponding to Reynolds numbers $Re_x = 1.56 \times 10^4$ and 1.88×10^5, respectively), and four different temperature differences between the heated surface and the free stream air: $\Delta T = 0\,^\circ\mathrm{C}$ (i.e., forced convection) and $\Delta T = 15, 30$, and $53\,^\circ\mathrm{C}$ (i.e., mixed convection), corresponding to Grashof numbers $Gr_x = 3.74 \times 10^9$, 6.61×10^9, and 9.81×10^9 at the streamwise location of 125 cm, and $Gr_x = 6.46 \times 10^9$, 1.14×10^{10}, and 2.65×10^{10} at the streamwise location of 150 cm. Fig. 8 illustrates the effect of wall heating (i.e., buoyancy force) on the streamwise velocity distributions. These figures indicate clearly that wall heating has only a small effect on the streamwise velocity distributions when the flow is stable and two-dimensional. This behavior is in sharp contrast with the case of vertical surface reported by Kitamura and Inagaki [16], Patel et al. [17], Abu-Mulaweh et al. [18], and Hattori et al. [19] where the buoyancy force affects significantly the streamwise velocity distributions. This is because in the vertical case the buoyancy force has a non-zero component in the streamwise direction in comparison to the horizontal case where the buoyancy force component in the streamwise direction is zero. Fig. 8 shows that the velocity profiles for heated turbulent boundary layer flows ($\Delta T = 15, 30$, and $53\,^\circ\mathrm{C}$) appear to deviate from the $1/7$th power law. This is because the flow is no longer two-dimensional due to the onset of vortex instability which breaks down the two-dimensional nature of the flow. As can be seen from the figure, for a given free stream velocity at a given streamwise location this deviation increases as the temperature difference between the heated plate and the free stream increases. This is because increasing the temperature difference causes the onset/start of vortex instability to move closer the leading edge (i.e., smaller downstream distances from the leading edge) of the heated plate which allows the vortices to develop and grow in size. Also, the figure shows that for a given temperature difference between the heated plate and the free stream at a given streamwise location the deviation of the velocity profiles from the $1/7$th power law is larger for lower free stream velocities. This is because higher free stream velocities tend to move the onset/start of vortex instability further away from the leading edge (i.e., larger downstream distances from the leading edge) of the heated plate.

Instantaneous velocity fluctuation, u', from the time-mean streamwise velocity was deduced from the measured results in the boundary layer for different free stream velocities and different plate temperatures at different axial locations. The dimensionless turbulent intensities of streamwise velocity fluctuations are presented in Figs. 9, 10, and 11. The uncertainty in the measurements are ± 0.1 mm in y and $\pm 4\%$ in $\sqrt{\overline{u'^2}}/u_\infty$. As can be seen from these figures, the value of the streamwise velocity fluctuation increases to a maximum as the distance from the heated wall increases, starts to decrease as the distance from the heated wall continues

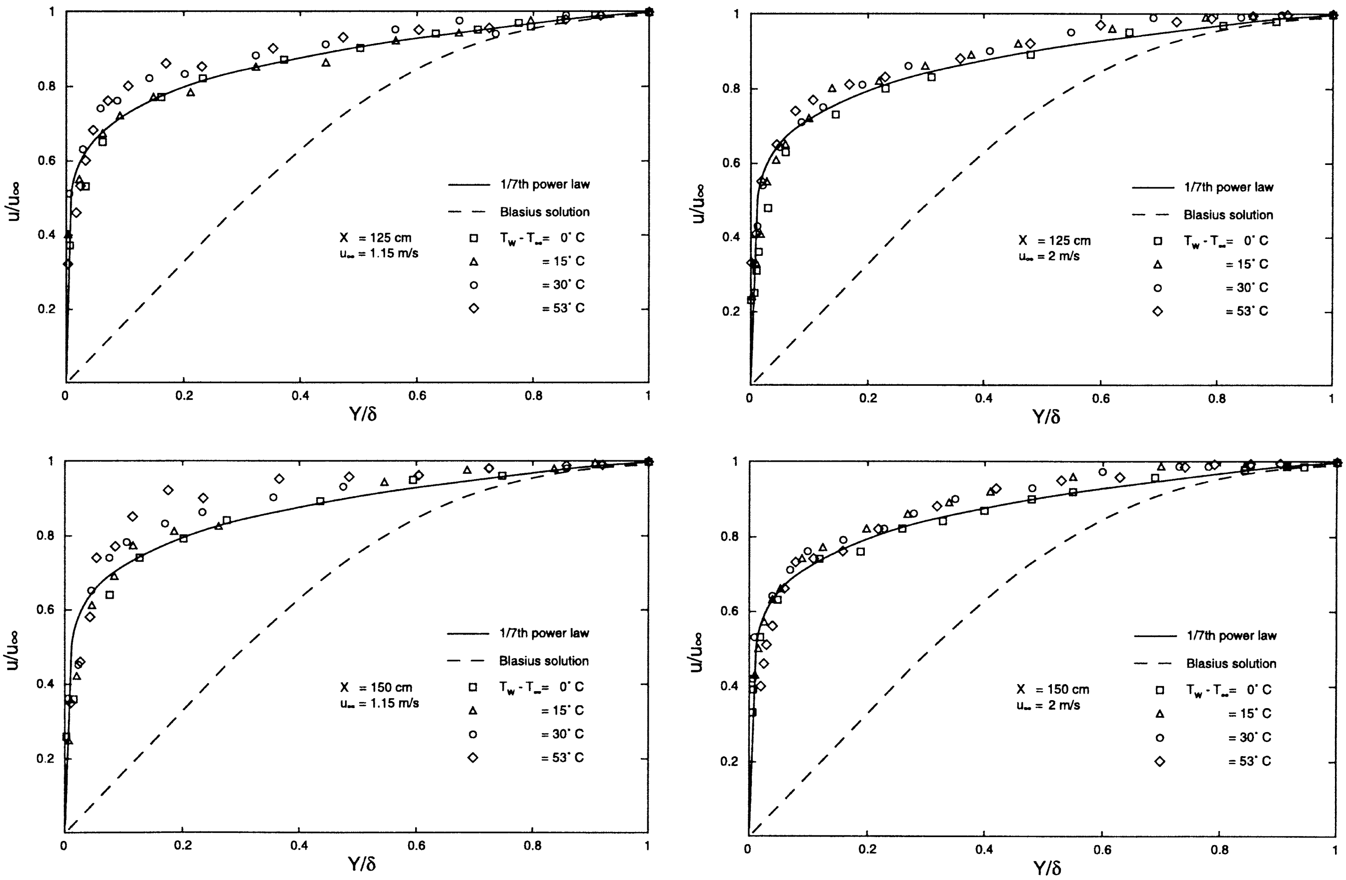

Fig. 8. Effect of heating on velocity distributions.

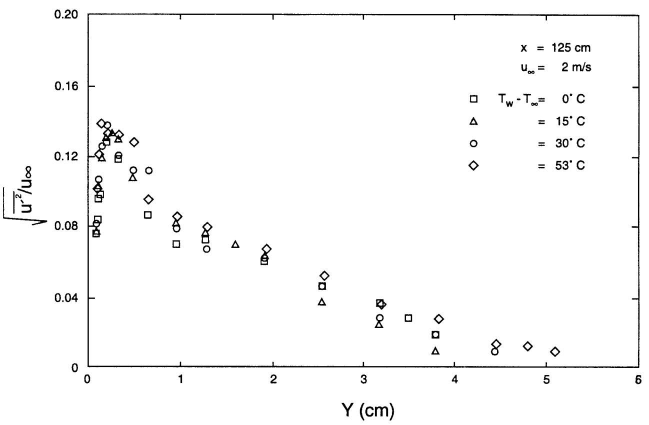

Fig. 9. Effect of heating on turbulence intensity.

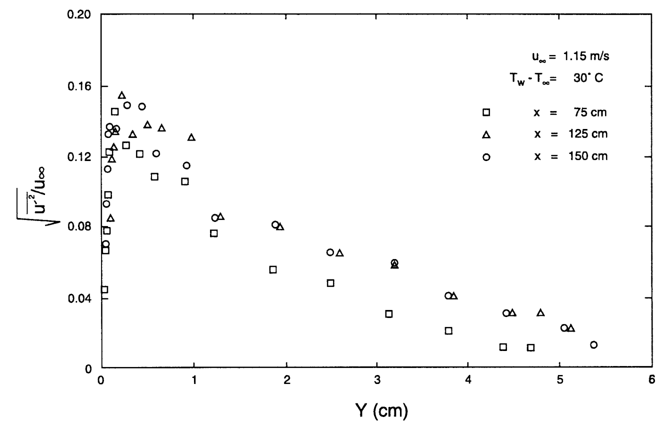

Fig. 10. Effect of streamwise location on turbulence intensity.

to increase, and then reach a minimum value at the edge of the boundary layer. Fig. 9 illustrates the effect of wall heating on the turbulent intensity of the streamwise velocity fluctuations at $x = 125$ cm for $u_\infty = 2\ \mathrm{m\cdot s^{-1}}$ and four different values of temperature difference between the plate and the free stream ($\Delta T = 0, 15, 30, 53\,^\circ\mathrm{C}$). It can be seen from this figure that the heated turbulent flow possesses a slightly different turbulent intensity distribution than the unheated turbulent flow. The figure also shows that the hydrodynamic boundary layer thickness increases with increasing wall heating. The measured turbulent intensity at three different axial locations ($x = 75, 125, 150$ cm), for a free stream velocity $u_\infty = 1.15\ \mathrm{m\cdot s^{-1}}$ and a temperature difference $(T_w - T_\infty) = 30\,^\circ\mathrm{C}$ is shown in Fig. 10. As can be seen from the figure, the turbulent intensity of the streamwise velocity fluctuation increases as the distance from the trip wire increases. Also, it can be seen from the figure, as expected, the hydrodynamic boundary layer thickness increases as the distance from the trip wire increases. The effect of free stream velocity on the turbulent intensity is

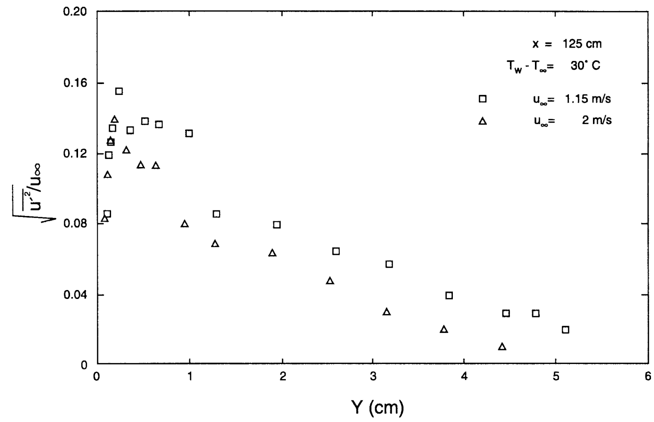

Fig. 11. Effect of free stream velocity on turbulence intensity.

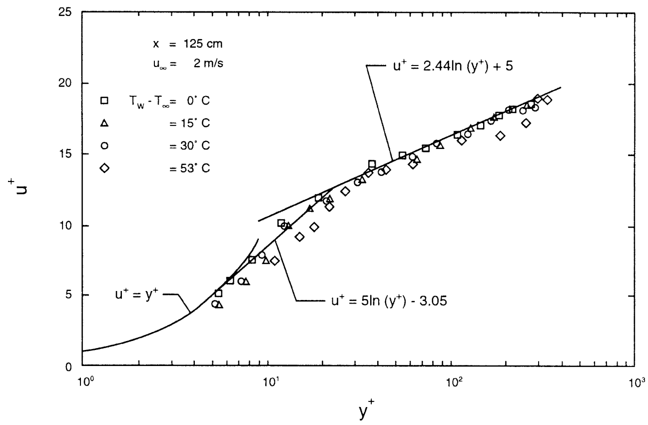

(a)

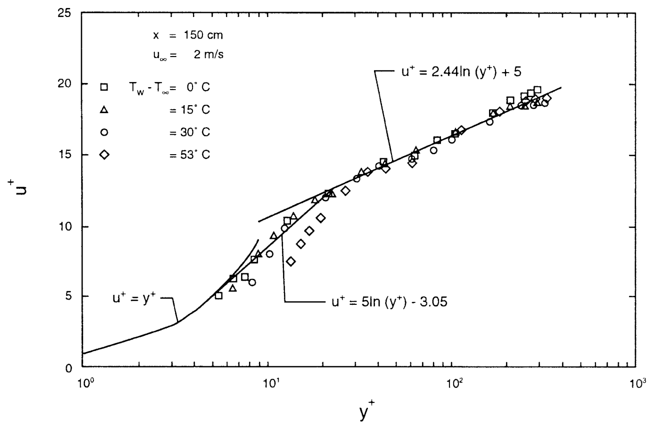

(b)

Fig. 12. Turbulent velocity profiles u^+ versus y^+: (a) $x = 125$ cm, (b) $x = 150$ cm.

shown in Fig. 11. The figure clearly shows that the turbulent intensity of the streamwise velocity fluctuation decreases as the free stream velocity increases. The figure also shows that the hydrodynamic boundary layer thickness decreases as the free stream velocity increases.

The measured velocity profiles in the turbulent boundary layer for both heated and unheated plates at $x = 125$ and 150 cm for a free stream velocity of 2 m·s^{-1} are shown, respectively, in Figs. 12(a) and (b). The universal velocity profiles are also shown in solid lines in the figure by the following set of equations:

Laminar sublayer:

$$0 < y^+ < 5, \quad u^+ = y^+$$

Buffer layer:

$$5 \leqslant y^+ \leqslant 30, \quad u^+ = 5\ln(y^+) - 3.05 \tag{4}$$

Turbulent core:

$$y^+ > 30, \quad u^+ = 2.44\ln(y^+) + 5$$

The $u^+(y^+)$ expression for the turbulent core is taken from Kays and Crawford [20]. In the present study it was determined that at the axial location $x = 150$ cm for a free stream velocity of 2 m·s^{-1} the laminar sublayer extends up to $y = 0.75$ mm normal to the plate surface and the buffer layer extends from $y = 0.75$ up to $y = 4.5$ mm. The figures clearly show that for the unheated turbulent boundary layer, the experimental data agree with the universal velocity profiles. From the experimental study of Cheng et al. [7] it was established that the turbulent velocity profiles in the buffer layer and the turbulent core region depend on the temperature difference between the plate and the free stream. The turbulent velocity profiles tend to deviate from the universal velocity profiles as the temperature difference between the plate and the free stream increases. In the present study, this behavior is clearly exhibited in the buffer layer, but not so in the turbulent core region. The different profiles for different amount of heating are due to buoyancy effects. From the definition of $u^+ = u/u^*$ and the definition of $u^* = (\tau_w/\rho)^{1/2}$, one obtains $\tau_w = \rho(u/u^+)^2$, from which the local wall shear stress for turbulent mixed convection can be evaluated using Fig. 12. The uncertainty in the measured u^+ is $\pm 6\%$ and $\pm 5\%$ in y^+.

The friction velocity $u^* = (\tau_w/\rho)^{1/2}$ that appears in the definitions of u^+ and y^+ can be related to the friction factor C_f as $u^* = u_\infty(C_f/2)^{1/2}$. From $u^+ = u/u^*$ and $y^+ = yu^*/\nu$ one obtains $u^+ = (u/u_\infty)(2/C_f)^{1/2}$ and $y^+ = (u_\infty y/\nu)(C_f/2)^{1/2}$. In the turbulent core region the dimensionless logarithmic universal velocity distribution is given by $u^+ = 2.44\ln(y^+) + 5$. By relating u^+ to $(u/u_\infty)(2/C_f)^{1/2}$ and y^+ to $R_y(C_f/2)^{1/2}$, with $R_y = u_\infty y/\nu$, the above equation can be written as:

$$u/u_\infty = \left[2.44\ln\left(R_y(C_f/2)^{1/2}\right) + 5\right]/(2/C_f)^{1/2} \tag{5}$$

This relation was used to generate the u/u_∞ versus R_y plots for a fixed value of C_f as shown in Fig. 13. The measured velocity as a function of y for a given axial location x were then presented in terms of u/u_∞ versus R_y and the appropriate value of C_f was obtained by selecting the analytical curve that provided the best fit with the measured data. From this technique, as can be seen from the figure, the experimental friction factor C_f was found to be about 0.006 for a typical set of data.

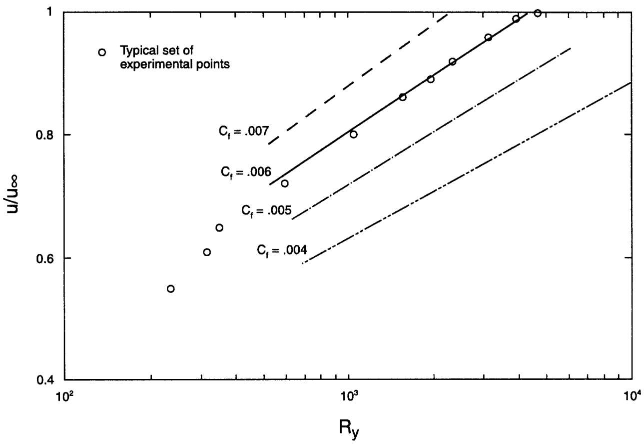

Fig. 13. Experimental turbulent skin friction.

4. Conclusion

Turbulent mixed convection boundary layer flow resulting from the use of a trip wire over a horizontal flat plate was investigated experimentally. As expected, the trip wire did accelerate the transition of laminar boundary layer flow to a fully developed turbulent boundary layer flow. Measured velocity profiles indicate a significant departure from the Blasius profile and a clear approach to the $1/7$th power law for fully developed turbulent flow. The results reveal that the buoyancy force resulting from wall heating has negligible effect on the flow field as long as the flow is stable. This is because the buoyancy force has no streamwise component in the case of horizontal heated flat plate. However, it influences significantly the onset/start of vortex instability.

References

[1] S.P.S. Arya, Buoyance effects in a horizontal flat-plate boundary layer, J. Fluid Mech. Part 2 68 (1975) 321–343.

[2] M.Y. Chung, H.J. Sung, Four-equation turbulence model for prediction of turbulent boundary layer affected by buoyancy force over a flat plate, Internat. J. Heat Mass Transfer 27 (1984) 2387–2395.

[3] J.L. Lumley, O. Zeman, The influence of buoyancy on turbulent transport, J. Fluid Mech. Part 3 84 (1978) 581–596.

[4] N. Ramachandran, B.F. Armaly, T.S. Chen, Turbulent mixed convection over an isothermal horizontal flat plate, ASME J. Heat Transfer 112 (1990) 124–128.

[5] A.A. Townsend, Mixed convection over a heated horizontal plane, J. Fluid Mech. Part 2 24 (1972) 209–227.

[6] H. Imura, R.R. Gilpin, K.C. Cheng, An experimental investigation of heat transfer and buoyancy induced transition from laminar forced convection to turbulent free convection over a horizontal isothermally heated plate, ASME J. Heat Transfer 100 (1978) 429–434.

[7] K.C. Cheng, T. Obata, R.R. Gilpin, Buoyancy effects on forced convection heat transfer in the transition regime of horizontal boundary layer heated from below, in: Proceedings of ASME Winter Annual Meeting, Anaheim, California, December 7–12, ASME Paper 86-WA/HT-97, 1986.

[8] J.J. Miau, M.H. Chen, Flow structures behind a vertically oscillating fence immersed in a flat-plate turbulent boundary layer, Experiments Fluids 11 (1991) 118–124.

[9] I. Ziugzda, Y.L. Tonkonogiy, Generation of turbulence by means of a longitudnal baffle in a flow with a low Reynolds number in a flat duct, Heat Transfer Soviet Res. 23 (1991) 884–891.

[10] M.O. Carpinlioglu, Comments on the turbulent wake growth behind an isolated spherical roughness element, Modeling, Measurement & Control B: Solid & Fluid Mechanics & Themes, Mechanical Systems 59 (1995) 37–43.

[11] M.W. Pinson, T. Wang, Effects of leading-edge roughness on fluid flow and heat transfer in the transitional boundary layer over a flat plate, Internat. J. Heat Mass Transfer 40 (1997) 2813–2823.

[12] H.I. Abu-Mulaweh, B.F. Armaly, T.S. Chen, Measurements of laminar mixed convection flow over a horizontal forward-facing step, J. Thermophys. Heat Transfer 7 (1993) 569–573.

[13] R.J. Moffat, Describing the uncertainties in experimental results, Exp. Therm. Fluids Sci. 1 (1988) 3–17.

[14] J.P. Holman, Heat Transfer, 8th Edition, McGraw-Hill, New York, 1997, pp. 203–204.

[15] S. Moharreri, B.F. Armaly, T.S. Chen, Measurements in the transition vortex flow regime of mixed convection above a horizontal heated plate, ASME J. Heat Transfer 110 (1988) 358–365.

[16] K. Kitamaura, T. Inagaki, Turbulent heat and momentum transfer of combined forced and natural convection along a vertical flat plate — aiding flow, Internat. J. Heat Mass Transfer 30 (1987) 23–41.

[17] K. Patel, B.F. Armaly, T.S. Chen, Transition from turbulent natural to turbulent forced convection, ASME J. Heat Transfer 120 (1998) 1086–1088.

[18] H.I. Abu-Mulaweh, T.S. Chen, B.F. Armaly, Effects of free stream velocity on turbulent natural convection flow along a vertical plate, Experimental Heat Transfer 13 (2000) 183–195.

[19] Y. Hattori, T. Tsuji, Y. Nagano, N. Tanaka, Effects of freestream on turbulent combined-convection boundary layer along a vertical heated plate, Internat. J. Heat Fluid Flow 22 (2001) 315–322.

[20] W.M. Kays, M.E. Crawford, Convective Heat and Mass Transfer, 3rd Edition, McGraw-Hill, New York, 1993, p. 172.